Correspondence between Phase Resolved Partial Discharge Patterns and Corona Discharge Modes

Zhicheng Wu, Qiaogen Zhang, Zhehao Pei and **Heli Ni**
State Key Laboratory of Electric Insulation and Power Equipment
Xi'an Jiaotong University
Xi'an, 710049, P. R. China

ABSTRACT

Corona discharge under super low frequency (30-300 Hz) voltage is common in high-voltage transmission lines and equipment. The phase resolved partial discharge (PRPD) pattern is the most commonly used tool for power equipment condition-monitoring in the electrical engineering field. The present study centers on the correspondence between PRPD patterns and corona discharge modes under a wide range of applied voltage. Electric and optical emission characteristic measurement methods are applied to obtain PRPD patterns and phase resolved discharge images. The transition of corona discharge types and space charge behavior under different applied voltage are investigated. The electric field generated by negative needle electrode is shown to erase residual positive ions, which leads to an abundance of positive streamer bursts when applied voltage is low. Once the negative glow corona emerges under higher applied voltage, dense positive ions in the cathode sheath suppress the positive streamer bursts. The existence of residual positive ions is crucial for the transition from positive streamer discharge to glow corona discharge. A comprehensive understanding of PRPD patterns may help electrical engineers to assess the threat of partial discharge of the power equipment correctly.

Index Terms — **partial discharges, corona, condition monitoring**

1 INTRODUCTION

CORONA discharge under super low frequency (SLF) (between 30 Hz and 300 Hz) voltage is common in high-voltage transmission lines and equipment [1]. Corona discharge is commonly utilized for surface modification [2], gas treatment [3, 4], electrohydrodynamic (EHD) spraying [5], and solid-state fan [6] applications; it is easily and conveniently implemented in air atmospheres. Alternating current (AC) voltage, especially SLF voltage, is a commonly used discharge excitation. Phase-dependent characteristics can be exploited to analyze various discharge properties. For example, the phase resolved partial discharge (PRPD) pattern is a commonly used tool for power equipment condition-monitoring in the electrical engineering field.

In a 1956 study, Brown investigated the breakdown discharge in gases under an alternating electric field; he treated discharge characteristics as independent of voltage frequency if the positive ions all enter the electrode due to the removed space charge [7]. Based on this theory, the discharge under SLF voltage should be similar to that under DC voltage in a centimeter-size air gap. Corona discharge characteristics under SLF voltage were once considered fully equivalent to direct current DC excitation, because the time scale of applied voltage markedly differs from the time scale of transient discharge.

The differences between the discharges under SLF voltage and DC voltage were identified by Van Brunt in 1982. He compared the corona inception voltage between a 60 Hz AC voltage and DC voltage of SF_6 gas; various types of negative ions proved able to survive prior to polarity reversal due to their lower mobility in high electronegative gas pressure [8]. In 2014, Piccin found that "memory effect" is lost if the time elapsed between two consecutive discharges is greater than the time required to the space charge to drift away [9]. He studied pulse height distribution, q-U, and other corona discharge characteristics between 50 Hz AC voltage and DC voltage [10]. By 1991, Chang had divided the corona discharge into three or four type in the case of positive or negative DC voltage [3]. Researchers and developers have recognized clear boundaries separating corona discharge characteristics under different excitation modes, but few have investigated the precise effects of corona discharge modes. In this study, PRPD patterns were utilized to investigate transitions in corona discharge types.

The present study centers on the correspondence between PRPD patterns and corona discharge modes. Electric and

Manuscript received on 29 September 2018, in final form 28 October 2018, accepted 5 November 2018. Corresponding author: Z. Wu.

DOI: 10.1109/TDEI.2018.007855

optical emission characteristic measurement methods are introduced in Section 2. PRPD patterns and phase resolved discharge images are presented in Section 3. Transitions in corona discharge types and space charge behavior under different applied voltages are discussed in Section 4. A comprehensive understanding of PRPD patterns may help electrical engineers to correctly assess the threat of partial discharge in power equipment.

2 EXPERIMENTAL SETUP

A needle-plane electrode system was used to determine the corona discharge characteristics in an air atmosphere. The needle electrode is a hemispherical-capped cylinder with a curvature radius of 500 μm; the gap distance was set to precisely 20 mm. The needle electrode and plane electrode were made of stainless steel. The calculated electric field uniformity coefficient, 27.8, formed a typical extremely inhomogeneous electric field. The experiment was carried out in room air, and the temperature and humidity were 25 C and 40%, respectively. The breakdown voltage of this electrode system is 20.4 kV·rms at the positive half cycle peak, so we focused on the corona discharge characteristics under applied voltages ranging from 8 to 18 kV. The root mean square (rms) is used here to describe the applied voltage unless otherwise specified.

Several measurement methods were applied (Figure 1) to assess corona discharge characteristics. Electrical characteristics including voltage, current, and apparent charge signals were collected and a Tektronix® P6015A 1000× high-voltage probe was used to measure voltage waveshape [11, 12]. A non-inductive resistor (50 Ω), regarded as a shunt, was connected with the plane electrode to measure the current. According to standard IEC 60270 [13], the apparent charge of corona discharge was measured by a coupling capacity and a measurement impedance in parallel with the needle-plane electrode system. The PRPD patterns were obtained by with a partial discharge detector (Techimp® PDCheck). We also measured optical emission characteristics, as mentioned above. Phase synchronization photography was used to assess spatial resolution as per the AC discharge; phase resolved discharge images were captured with a phase synchronized device (PSD) [14] and single lens reflex camera (Nikon® D5) with an exposure time of 2.5 s and photosensitivity of ISO-102400. The photoelectric signal was captured by a photomultiplier tube (PMT), Hamamatsu® CR131 (Effective area: 24 × 8 mm/Spectral response: 185 to 900 nm) through the focusing lens to determine temporal resolution. The voltage applied to the cathode and the anode of PMT was -900 V throughout this experiment. All signals were recorded by a digital oscilloscope (Tektronix® MDO3102) with a bandwidth of 100 MHz.

3 RESULTS

We obtained PRPD patterns and phase resolved discharge images for the purposes of this study. Corona discharge behavior is strongly related to the applied voltage, so we focused on the corona discharge characteristics from the inception voltage and breakdown voltage. Discharge mode transitions can be identified according to this information.

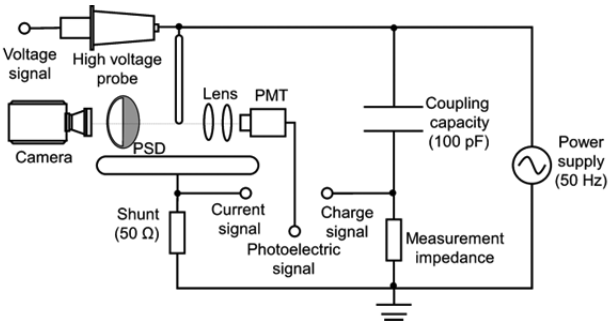

Figure 1. Schematic diagram of the experimental setup.

3.1 PRPD PATTERNS

The various discharges under different applied voltages are presented in polar diagram form in Figure 2. The phase-dependent characteristics of different half cycles differ and are sensitive to the applied voltage.

At the positive half cycle, strong discharge pulses appear at a stable voltage phase under the specific applied voltage. The phase decreases as the applied voltage increases. This burst phase θ can be expressed by the streamer inception voltage U_{IV} and the peak value of applied voltage $\hat{U}$ (Equation (1)) [15]. These burst pulses are the first discharge in the positive half cycle. No discharge pulse signals were observed in the positive half cycle except for these burst pulses. Sparse bursts indicate a decrease in burst probability at higher voltages. The apparent charge decreases almost linearly as the applied voltage increases. No burst pulses were observed once the applied voltage reached 16 kV, and no pulse appeared after the streamer bursts even at the voltage peak,

$$\theta = \arcsin\left(\frac{U_{\mathrm{IV}}}{\hat{U}}\right) . \tag{1}$$

At the negative half cycle, the discharges at negative polarity grow more frequent and almost symmetrical with the voltage peak in cases where the applied voltage is close to the inception voltage. The apparent charge of these pulses decreases slightly as the applied voltage increases. The apparent charge of the pulses which appear at the voltage peak is lower than other phases in the case of higher applied voltage ($U \geq 14$ kV); the repetition rate is lower, as well. That is, the pattern shows a doublet shape. This phenomenon is notable as it is contrary to common sense.

In summary, the PRPD patterns of corona discharge under small electrical stress are similar to those obtained by previous researchers [16-18], i.e., the apparent charge of positive polarity discharges is large and repetition rate is low. These characteristics are compeletely opposite in the case of negative polarity discharge. Abnormal phenomena under higher electric excitation are noteworthy: the vanished positive polarity discharge and is faint negative polarity discharge at the voltage peak are particularly unusual.

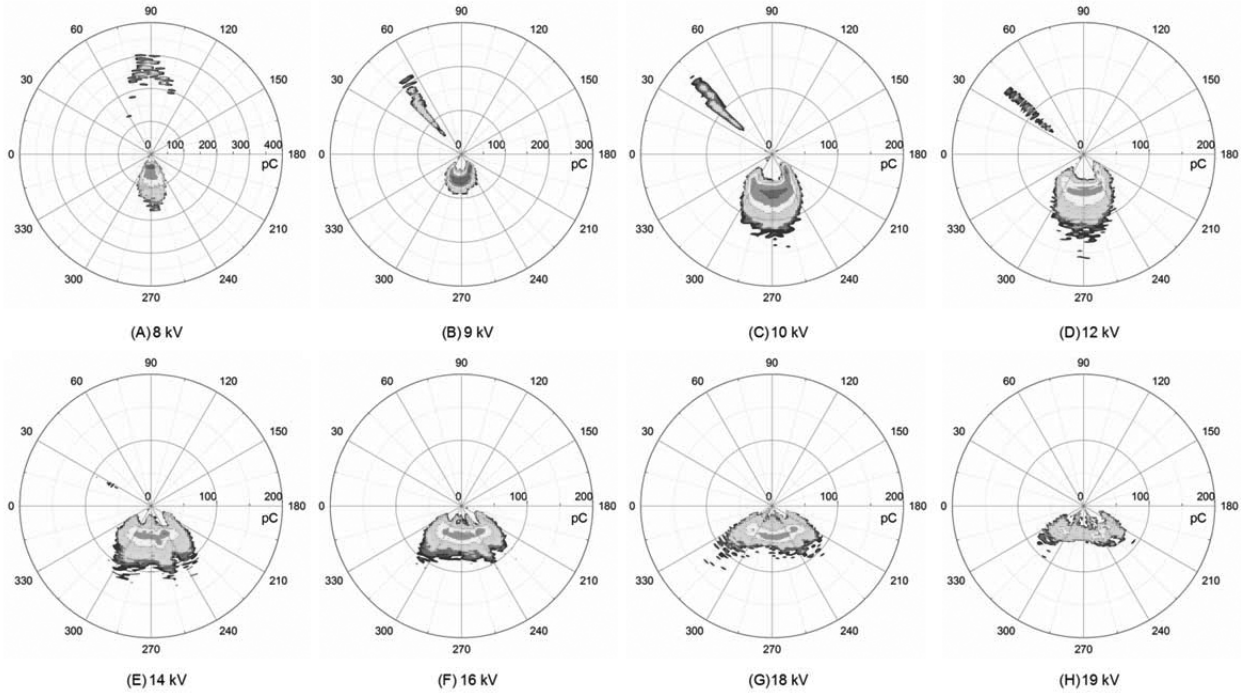

Figure 2. PRPD patterns under different applied voltage. Color represents discharge frequency.

3.2 PHASE RESOLVED DISCHARGE IMAGES

The overlapping discharge images were divided into phase-resolved discharge images via phase synchronized photography [14] to investigate the correspondence between PRPD patterns and discharge images. Discharge images in the positive half cycle and negative half cycle under different applied voltages are shown in Figure 3. We observed entirely disparate corona discharge appearances in different half cycles. As the applied voltage increases, the corona discharge type in the positive half cycle changes from positive streamer discharge with several filaments along the electric field line to a glow corona discharge with a uniform illuminant region surrounding the electrode [19]. As applied voltage increases from 8 to 14 kV, the positive streamer discharge coning angle decreases from 180° to 90° and the streamer length shortens. The largest volume discharge forms at 8 kV, where the streamer filaments extend to the plane electrode. We infer that the streamer channels which decreased with increasing applied voltage are related the burst discharge pulses at the positive half cycle. The volume of the glow corona discharge increases slightly when applied voltage increases from 16 to 18 kV. The corona discharge in the negative half cycle is diffuse and with an unclear boundary. The volume of the corona discharge increases as applied voltage increases. The gap is almost entirely illuminated by corona discharge when the applied voltage reaches 16 kV.

The phase resolved characteristics of electric characteristics and optical emission characteristics are strongly associated. For example, the vanished burst pulses seem related to the vanished positive streamer channels as the applied voltage increases. The apparent causes of these phenomena are discussed below.

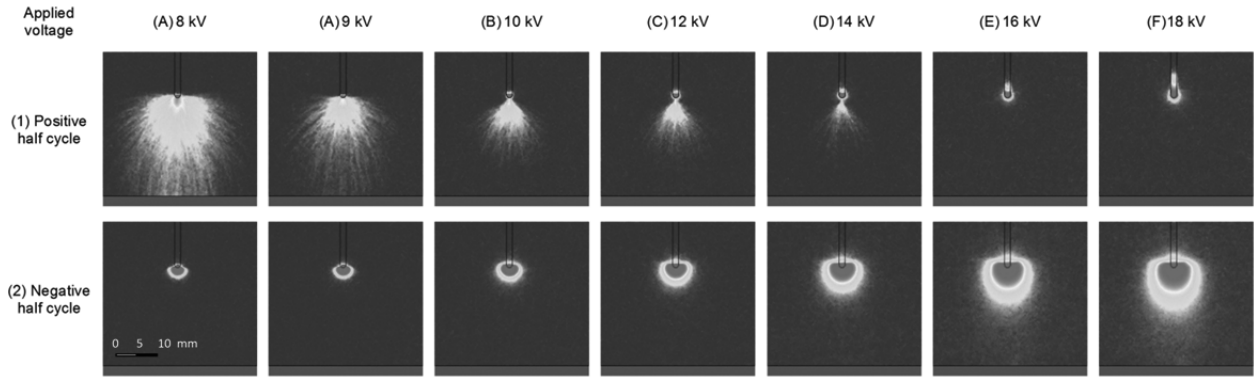

Figure 3. Phase resolved discharge images under different applied voltages as-obtained via phase synchronized photography.

4 DISCUSSION

The presence or absence of positive filaments under different applied voltages is the focal point of this discussion. We compared the discharge images under DC voltage, SLF voltage, and impulse voltage to explore the effects of the space charge on discharge behavior. The interaction of discharges at each half cycle was considered the culprit of abnormal phenomena as per our analysis of the current/photoelectric signalThe discharge images in the positive half cycle were compared with the results under positive DC voltage (Figure 4A)) and positive impulse voltage (Figure 4B [20]). Discharge images with applied voltages of 8, 10, 16, and 24 kV positive DC voltage are shown in Figure 4a. Under positive DC voltage, no further streamer channels appear once the applied voltage reaches 10 kV; a glow corona discharge replaces the streamer discharge at slightly higher voltage. Only a few faint stream channels can be seen in a small volume near the needle electrode at 8 kV. On the contrary, the streamer discharge spreads across a wider voltage range as the major discharge type under SLF voltage. Discharge images with an exposure time of 100 ns and an applied 30 kV positive impulse voltage (standard lightning impulse voltage, T_f = 1.2 μs, T_t = 50 μs) were captured by a MCP-image intensifier camera (PCO.® HSFC with a spectral response of 380 to 900 nm) for comparison as shown in Figure 4B. There are streamer channels emanating from the needle electrode which appear similar to those captured under low SLF voltage.

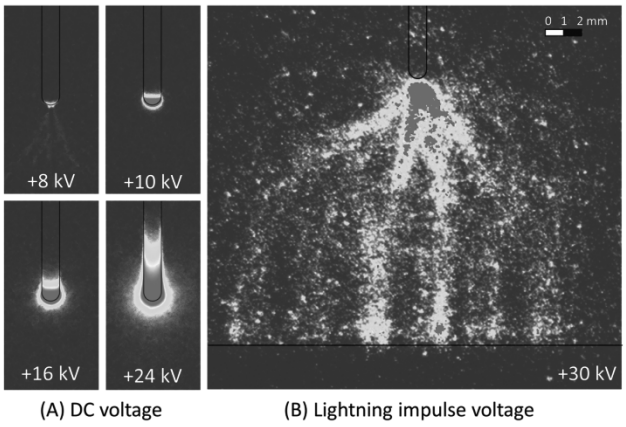

Figure 4. Discharge images under positive DC voltage and positive impulse voltage.

The discharge under an impulse voltage with a brief front time can be considered independent of space charge, but space charge plays a vital role in discharge under a steady-state voltage such as DC or SLF. We observed a stream discharge in the case of impulse voltage as opposed to DC voltage. In the case of DC, the residual positive ions generated by previous positive streamers can weaken the electric field strength, resulting in the absence of subsequent streamer bursts. The necessary condition for positive streamer discharge is a sufficiently low background positive ion density. The positive streamer discharge burst is a major discharge in the case of SLF voltage, wherein the negative half cycle plays an important role. This streamer discharge is the first discharge pulse in the positive half cycle as we discussed in Section 3.1. So the residual positive ions generated by a previous positive streamer discharge can be removed effectively by the negative half cycle, thus the positive streamer burst is a common phenomenon under low SLF voltage.

Another abnormal phenomena is the glow corona discharge which replaces the stream discharge at higher SLF voltage, even if the positive ions can be removed by the negative half cycle electric field. Typical current and photoelectric signals under applied voltages of 9 and 19 kV are shown in Figure 5. A positive streamer burst is inevitable once the applied voltage exceeds the inception voltage — only one burst pulse with a high current amplitude appears per positive half cycle in our image and is accompanied by a strong photoelectric signal (Figure 5A1). The abundance of streamer channels in the ICCD image (Figure 5A2) indicates that the current pulses correspond to positive streamer discharge bursts. Compared the second ICCD image in Figure 5 with Figure 4a, the discharge mode from the positive streamer burst to the end of the positive half cycle is similar to that under the DC voltage, under the influence of residual positive ions. That is, the glow corona discharge then becomes the dominant corona discharge

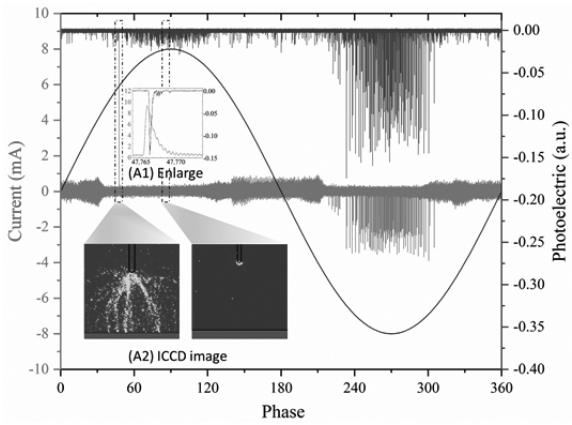

(a) 9 kV

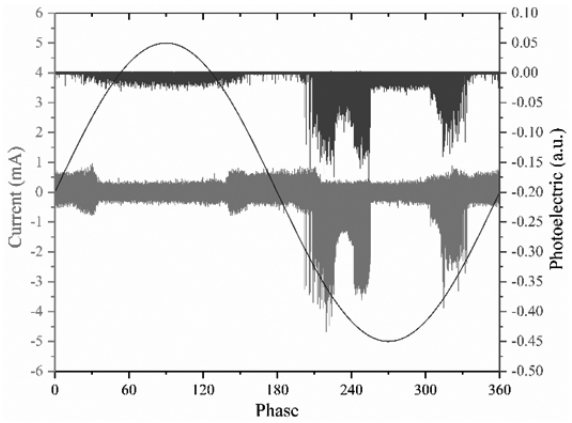

(b) 19 kV

Figure 5. Typical current signal and photoelectric signal under (a) 9 kV and (b) 19 kV, including enlarged and ICCD images (PCO® HSFC, exposure tbme: 100 ns).

mode without current pulses. In Figure 5a, the frequent photoelectric pulses without any current pulses also prove that the discharge mode is turning to glow discharge. The current signal and photoelectric signal in the negative half cycle are homologous and continuous.

As shown in Figure 5b, the streamer burst current pulse next disappears and the pulses in the negative half cycle become discontinuous. The corona discharge does not entirely cease – the photoelectric signal shows light emission pulses regardless of positive half cycle or negative half cycle discontinuities. What had actually occurred at this point is a transition in discharge type. The Trichel discharge transformed into a negative glow corona discharge once the instantaneous voltage approached the voltage peak [21, 22]. The current pulses were difficult to detect due to the DC component of the negative glow corona discharge, which accounts for the abnormal negative half cycle phenomenon shown in Figure 2.

We infer that positive streamer discharge burst and negative discharge onset exhibit contrary phenomena as applied voltage increases. The current signal and photoelectric signal of 20 cycles at each applied voltage were observed to evaluate the probabilities of positive streamer burst and nagative glow corona inception. We appreciate that you mentioned this negligence. The criterion for judging the occurrence of positive streamer burst is whether a current pulse greater is than 2 mA appears in the positive half cycle with a strong photoelectric signal. And the criterion of negative glow corona is whether an intermittent duration of current pulses in negative half cycle exceeds 2 ms. The relationship between the probabilities of these two phenomena and the applied voltage is shown in Figure 6. The positive streamer burst disappears upon the onset of a negative corona discharge. In other words, a negative glow corona discharge prevents any positive streamer discharge burst. The existence of a negative glow corona discharge can weaken the electric field in front of the needle electrode due to the dense positive ions in cathode sheath, according to the space charge structure of negative glow discharge [23, 24]. After negative glow corona discharge occurs in the negative half cycle, positive ions are generated rather than removed. A higher positive ion density then suppresses the occurrence of positive stream bursts.

The electric field generated by the negative needle electrode can erase residual positive ions, leading to an abundance positive streamser bursts, in the case of lower applied voltage. Once the negative glow corona emerges under higher applied voltage, the dense positive ions in the cathode sheath suppress the occurrence of positive streamer bursts. The existence of residual positive ions is crucial for the transition from positive streamer discharge to glow corona discharge.

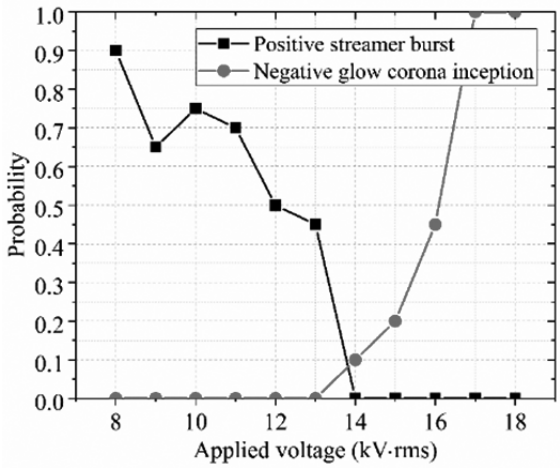

Figure 6. Probabilities of positive streamer burst and negative glow corona inception as a function of applied voltage.

5 CONCLUSIONS

This study was conducted to examine the correspondence between PRPD patterns and corona discharge modes according to electric and optical emission characteristics. Our results can be summarized as follows:

1) The PRPD patterns and phase resolved discharge images under increasing applied voltage reveal transitions in corona discharge modes. At the positive half cycle, strong discharge pulses appear at a stable voltage phase under the specific applied voltage under low applied voltage; these pulses disappear under higher applied voltages. At the negative half cycle, the apparent charges of pulses which appear at the voltage peak are lower than other phases in the case of higher applied voltage. The corona discharge mode under high applied voltage differs markedly from that under low applied voltage.
2) Overlapping discharge images were divided into phase-resolved discharge images via phase synchronized photography. it can be observed entirely disparate corona discharge appearances in different half cycles. As the applied voltage increases, the corona discharge type in the positive half cycle changes from a positive streamer discharge with several filaments along the electric field line to a glow corona discharge with a uniform illuminant region surrounding the electrode. The corona discharge in the negative half cycle is diffuse and with an unclear boundary.
3) The electric field generated by a negative needle electrode can erase residual positive ions, leading to an abundance of positive streamer bursts when applied voltage is low. Once the negative glow corona emerges under higher applied voltage, the dense positive ions in the cathode sheath suppress the occurrence of positive streamer bursts. The existence of residual positive ions is crucial for the transition from positive streamer discharge to glow corona discharge.

From the perspective of condition monitoring of air-insulated power equipment, the severity of the defects can be evaluated by measuring the PRPD pattern. For example, once the negative discharge pattern shows a doublet shape, it can be infered that this defect is about to breakdown and should be disposed immediately. This paper may help electrical engineers to assess the threat of partial discharge of the power equipment correctly.

REFERENCES

[1] R. G. Olsen, M. W. Tuominen, and J. T. Leman, "On corona testing of high voltage hardware using laboratory testing and/or simulation," IEEE Trans. Power Del., vol. 33, no. 4, pp. 1707–1715, 2017.

[2] M. Strobel *et al*, "A comparison of corona-treated and flame-treated polypropylene films," Plasmas and Polymers, vol. 8, no. 1, pp. 61–95, 2003.

[3] M. Abdel-Salam, M. Th. El-Mohandes, and S. Kamal El-deen, "Analysis of corona discharge in wire-cylinder ESP with and without particle loading, " IEEE Trans. Dielectr. Electr. Insul., vol. 23, no. 5, pp. 2607–2616, 2016.

[4] J. Chang, P. A. Lawless, and T. Yamamoto, "Corona discharge processes," IEEE Trans. Plasma Sci., vol. 19, no. 6, pp. 1152–1166, 1991.

[5] Z. Feng, Z. Long, and K. Adamiak, "Numerical simulation of electrohydrodynamic flow and vortex analysis in electrostatic precipitators," IEEE Trans. Dielectr. Electr. Insul., vol. 25, no. 2, pp. 404–412, 2018.

[6] W. Qiu, L. Xia, X. Tan, and L. Yang, "The velocity characteristics of a serial-staged ehd gas pump in air," IEEE Trans. Plasma. Sci., vol. 38, no. 10, pp. 2848–2853, 2010.

[7] S. C. Brown*, Basic Data of Plasma Physics*, Press of the Massachusetts Institute of Technology, 1959.

[8] R. J. V. Brunt and M. Misakian, "Mechanisms for inception of DC and 60-Hz AC corona in SF_6," IEEE Trans. Dielectr. Electr. Insul., vol. 17, no. 2, pp. 106–120, 1982.

[9] R. Piccin, A. R. Mor, P. Morshuis, A. Girodet, and J. Smit, "Partial discharge analysis of gas insulated systems at high voltage AC and DC," IEEE Trans. Dielectr. Electr. Insul., vol. 22, no. 1, pp. 218–228, 2015.

[10] S. Zhang, B. Zhang, and J. He, "Comparison of direct current and 50 Hz alternating current microscopic corona characteristics on conductors," Phys. Plasmas, vol. 21, no. 6, pp. 063503, 2014.

[11] A. Kovacevic *et al*, "Uncertainty evaluation of the conducted emission measurements," Nucl. Technol. Radiat., vol. 28, no. 2, pp. 182–190, 2013.

[12] A. Kovacevic, A. Kovacevic, K. Stankovic, and U. Kovacevic, "The combined method for uncertainty evaluation in electromagnetic radiation measurement," Nucl. Technol. Radiat. Protection, vol. 29, no. 4, pp. 279 – 284, 2014.

[13] High-voltage Test Techniques – Partial Discharge Measurements, IEC Standard 60270: 2015, 2015-11-27.

[14] Z. Wu, Q. Zhang, J. Ma, and L. Pang, "Note: A phase synchronization photography method for AC discharge," Rev. Sci. Instrum., vol. 89, no. 5, pp. 056107, 2018.

[15] Z. Wu, Q. Zhang, J. Ma, X. Li, and T. Wen, "Effectiveness of on-site dielectric test of GIS equipment," IEEE Trans. Dielectr. Electr. Insul., vol. 25, no. 4, pp. 1454–1460, 2018.

[16] P. Osmokrovic *et al*, "Mechanism of electrical breakdown of gases for pressures from 10^{-9} to 1 bar and inter-electrode gaps from 0.1 to 0.5 mm," Plasma Source Sci. T., vol. 16, no. 3, pp. 643–655, 2007.

[17] M. Pejovic, M. Pejovic, and K. Stankovic, "Experimental investigation of breakdown voltage and electrical breakdown time delay of commercial gas discharge tubes," Jpn. J. Appl. Phys., vol. 50, no. 8, pp. 086001, 2011.

[18] Z. Rajovic, M. Vujisis, K. Stankovic, and P. Osmokrovic, "Influence of SF_6-N_2 gas mixture parameters on the effective breakdown temperature of the free electron gas," IEEE Trans. Plasma Sci., vol. 41, no.12, pp. 3659–3665, 2013.

[19] W. Hermstein, "Die entwicklung der positiven vorentladungen in luft zum durchschlag," Arch. Elektrotech., vol. 45, no. 4, pp. 279–288, 1959.

[20] C. Guo, "Study on synergetic effect of SF_6/N_2 gas mixtures under lightning impulse", PhD dissertation, State Key Laboratory of Electr. Insul. and Power Equip., Xi'an Jiaotong University, Xi'an, China, 2018.

[21] R. Morrow, "Theory of stepped pulses in negative corona discharges," Phy. Rev. A, vol. 32, no. 6, pp. 3821–3824, 1985.

[22] Y. Yang, W. Li, Y. Xia, and C. Yuan, "External characteristics of long gap AC and DC streamer discharges under low pressure," IEEE Trans. Dielectr. Electr. Insul., vol. 24, no. 6, pp. 3381–3387, 2017.

[23] Y. Zhang, Y. Qin, Z. Gao, and J. Ouyang, "Time-resolved analysis and optical diagnostics of Trichel corona in atmospheric air," J. Phys. D: Appl. Phys., vol. 49, no. 24, pp. 245206, 2016.

[24] Y. Zhang, X. Qing, Z. Jiang, and J. Ouyang, "Trichel pulse in various gases and the key factor for its formation," Scientific Report, vol. 7, no. 1, pp. 10135, 2017.

Zhicheng Wu (S'18) was born in Yunnan, China in 1993. He received a B.S. degree in computer science and technology from Xi'an Jiaotong University, Shaanxi, China in 2015. He is currently working toward a Ph.D. at the High Voltage Division, School of Electrical Engineering, and the State Key Laboratory of Electrical Insulation and Power Equipment. His research interest is technology for GIS/GIL defect detection.

Qiaogen Zhang received the B.S., M.S., and Ph.D. degrees in electrical engineering from Xi'an Jiaotong University, Xi'an, China, in 1988, 1991, and 1996, respectively. He is currently a Professor with the High Voltage Division, School of Electrical Engineering, and the State Key Laboratory of Electrical Insulation and Power Equipment, Xi'an Jiaotong University. His major research interests include insulation structure design, power transmission and transformation technology, and insulation state evaluation.

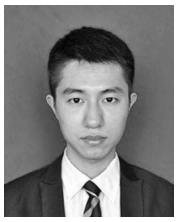

Zhehao Pei (S'18) received the B.Eng. degree from Xi'an Jiaotong University, Xi'an, China, in 2017, where he is currently pursuing the Ph.D. degree with the High Voltage Division, School of Electrical Engineering, State Key Laboratory of Electrical Insulation and Power Equipment.

Heli Ni was born in Jiangsu, China in 1993. He received the B.Sc. degree from the Xi'an Jiaotong University, Shaanxi, China in 2015. He is currently working toward the Ph.D. degree in the High Voltage Division, School of Electrical Engineering, and State Key Laboratory of Electrical Insulation and Power Equipment. His major research interests include oil-paper insulation and transient voltage distributions of windings.